

# 行政院國家科學委員會補助專題研究計畫成果報告

酵素型  $\text{WO}_3\text{-IrO}_2$  二極體陣列葡萄糖感測元件之可靠性研究

計畫類別：個別型計畫

計畫編號：NSC89-2215-E-009-087

執行期限：89年8月1日 - 90年10月31日

計畫主持人：趙書琦

本成果報告包括以下應繳交之附件：

赴國外出差或研習，心得報告一份

赴大陸地區出差或研習，心得報告一份

出席國際學術會議心得報告及發表之論文各一份

國際合作研究計畫國外研究報告書一份

執行單位：國立交通大學電子物理系

中華民國：90年10月26日

# 行政院國家科學委員會專題研究計畫成果報告

酵素型  $\text{WO}_3$ - $\text{IrO}_2$  二極體陣列葡萄糖感測元件之可靠性研究  
Reliability in enzymatic  $\text{WO}_3$  -  $\text{IrO}_2$  diode array microsensors for glucose

計畫編號：NSC89-2215-E-009-087

執行期限：89年8月1日 - 90年10月31日

主持人：趙書琦 研究助理：請見參考文獻<sup>19)</sup>

國立交通大學電子物理系

## 一、中文摘要

基於  $\text{WO}_3$  -  $\text{IrO}_2$  之類材料所組成的食物新鮮度感測器，會因為重覆的和固態食物樣品接觸，遭受磨損，而造成元件的可靠性下降。本計劃可以將，存在於元件上，機械強度較弱的環節 -  $\text{Ta}_2\text{O}_5$ 、酵素薄膜，在不妨礙元件電性的情況下，用  $\text{Ta}_2\text{O}_5/\text{Al}_2\text{O}_3$ 、鏈結酵素，加以取代，抵擋來自於樣品的磨損。此外， $\text{WO}_3$  -  $\text{IrO}_2$  二極體陣列，將予以二維化，以 redundancy 提昇元件的可靠性，並獲得生物分子的二維空間分佈資訊，邁入感測資訊影像化境界。

關鍵詞：可靠性、雙層抗干擾薄膜、表面修飾、鏈結酵素、二維陣列、二極體、微感測器、新鮮度、氧化鉭、氧化鋁、三氧化鎢、氧化鈹

## Abstract

In food freshness microsensors built from  $\text{WO}_3$  -  $\text{IrO}_2$ , abrasion of the device surface can arise due to repeated contacts with solid food samples. Particularly, the incorporation of other less durable components on the surface will severely limit device reliability. This investigation calls for the enhancement of reliability in the present device through three viable techniques. (1) Replace the previously used, mechanically weak  $\text{Ta}_2\text{O}_5$  by the abrasion-resistant  $\text{Ta}_2\text{O}_5/\text{Al}_2\text{O}_3$  bi-layer membrane to overcome the problem of interference. (2) Immobilize the enzyme covalently on the device surface to improve lifetime and overcome the problem of leaching in the previous device. (3) Expand the previous device into a 2-dimensional diode array. "Redundancy" will be built-in to allow the microsensor simultaneous, multiple measurements on a single food sample. This array can also be used to obtain spatially resolved, 2-dimensional imagery of glucose distribution in food samples.

Keywords : Reliability, Bi-layer, Surface Modification, Covalently Immobilized

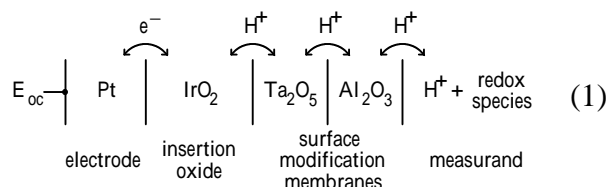
Enzyme, 2-Dimensional Array, Diode, Microsensor, Freshness,  $\text{Ta}_2\text{O}_5$ ,  $\text{Al}_2\text{O}_3$ ,  $\text{WO}_3$ ,  $\text{IrO}_2$

## 二、緣由與目的

This investigation calls for the enhancement of reliability in the present device through three viable techniques: (1) the use of an abrasion-resistant bi-layer membrane to combat the problem of interference; (2) immobilizing the enzyme covalently to prolong lifetime; and (3) expansion of the present device to a redundant 2-dimensional diode array. Due to their exceptional stability, insertion oxides (such as  $\text{WO}_3$ ,  $\text{IrO}_2$  and  $\text{Ni}(\text{OH})_2$ ) have attracted wide research interests. Unfortunately, in the case of food freshness microsensors built from insertion oxides, the incorporation of other less durable components can limit device reliability. Particularly, abrasion of the device surface can arise due to repeated contacts with solid food samples. To alleviate the problem, we propose to replace the previously used, mechanically weak  $\text{Ta}_2\text{O}_5$  and enzyme membrane by the abrasion-resistant  $\text{Ta}_2\text{O}_5/\text{Al}_2\text{O}_3$  and covalent attachment of the enzyme on the device surface. In addition, "redundancy" will also be built into the microsensor to allow simultaneous multiple measurements on one food sample. The measurements can thus be polled statistically to improve precision. To achieve this, the present device will be expanded to include rows of the linear arrays in a 2-dimensional layout. This array can also be used to obtain spatially resolved, 2-dimensional imagery of glucose distribution in food samples.

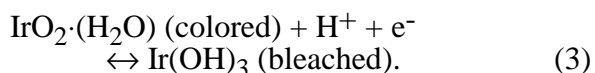
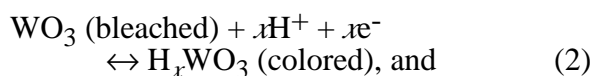
As mentioned before, a surface modification scheme employing the bi-layer  $\text{Ta}_2\text{O}_5/\text{Al}_2\text{O}_3$  membrane coated over the  $\text{WO}_3$  -  $\text{IrO}_2$  array to eliminate redox species interference is investigated this year. It is unfortunate that  $\text{WO}_3$  and  $\text{IrO}_2$  also conduct electronically. Microsensor arrays built with these exceptionally stable insertion oxides

will respond strongly to environmental redox species and suffer from interference errors in measurements. The conception of a Ta<sub>2</sub>O<sub>5</sub>/Al<sub>2</sub>O<sub>3</sub> membrane integrated over the surface of WO<sub>3</sub> - IrO<sub>2</sub> is based on the notion that Ta<sub>2</sub>O<sub>5</sub>/Al<sub>2</sub>O<sub>3</sub> are ionic conductor with electronic insulation. Use an IrO<sub>2</sub> electrode having its surface modified by Ta<sub>2</sub>O<sub>5</sub>/Al<sub>2</sub>O<sub>3</sub> as an example, the transport of carriers across the interfaces is:



Clearly, the membrane can mediate the transport of released protons from enzyme catalyzed reaction of glucose and block the transport of electrons from redox species. Insertion of protons by IrO<sub>2</sub> is not hindered whereas redox interference is eliminated. The conduction of both electrons and protons by insertion oxides can preserve the continuity of current<sup>1)</sup> without incidence in (1).

The present investigation is an expansion of the previous diode microsensor usable in resolving the glucose concentration gradient in food materials. It is constructed of single diodes that are operable in liquids at room temperature, Fig. 3. The previous diode device is based on pH-sensitive WO<sub>3</sub> and IrO<sub>2</sub>, which interact with H<sup>+</sup> in the reversible redox reactions,<sup>2,3)</sup>



Both WO<sub>3</sub> and IrO<sub>2</sub> reductions to the conducting H<sub>x</sub>WO<sub>3</sub> and insulating Ir(OH)<sub>3</sub> occur at more positive electrochemical potentials in acidic media over a range of pH values between ~2-12<sup>4,5)</sup> (reactions (2) and (3)). These redox transformations arise due to the insertion of ionic species into the oxides, which can produce large conductance changes.<sup>5,6)</sup> The present work is inspired by the earlier discoveries in this laboratory that a bicarbonate (HCO<sub>3</sub><sup>-</sup>)-doped, polyvinyl alcohol (PVA) solid polymer matrix interfaced with WO<sub>3</sub> or IrO<sub>2</sub>, can respond to CO<sub>2</sub> in terms of resistance or potential across closely spaced microelectrodes at 1 atm and room temperature.<sup>7,8)</sup> Despite the advantages

of such relatively simple chemical-sensitive resistors and potentiometers, practical use is less attractive due to the lack of a built-in current "turn-on" capacity commonly found in diode and transistor-based microsensors.<sup>9)</sup> However, WO<sub>3</sub> and IrO<sub>2</sub> are known to be complementary cathodic and anodic electrochromic materials,<sup>10)</sup> and have been used to demonstrate optical attenuation. By connecting WO<sub>3</sub> and IrO<sub>2</sub> in series, as shown in Fig. 3, both oxides become conducting under positive bias in the forward direction and insulating under negative bias in the reverse direction. However, the device function cannot be fully explained by treating the oxides simply as variable series resistors. Since H<sub>x</sub>WO<sub>3</sub>/WO<sub>3</sub> is cathodically electroactive whereas Ir(OH)<sub>3</sub>/IrO<sub>2</sub> is anodically electroactive, the transport of charge across the WO<sub>3</sub>/IrO<sub>2</sub> interface is allowed only in the forward direction and forbidden in the opposite direction. The current growth in the forward direction can occur readily via the thermodynamically favored reduction of IrO<sub>2</sub> by the reduced H<sub>x</sub>WO<sub>3</sub>. In fact, the attenuation of current in the reverse direction is more an indication that the oxidation of Ir(OH)<sub>3</sub> by the oxidized WO<sub>3</sub> is thermodynamically infeasible. In our view, this type of rectification governed by thermodynamic free energies is the major advantage for constructing such diodes based on the contact of WO<sub>3</sub> and IrO<sub>2</sub>. The devices will be durable since they are made of robust materials. Unlike previous microsensors based on conventional or organic diodes,<sup>9,11)</sup> their electrical functions in gases and liquids are not susceptible to the environmental variabilities arising from interfacial or material instability. Previous exploratory experiments in this area have led to our results<sup>12)</sup> that the electrical contacts of solid WO<sub>3</sub> and IrO<sub>2</sub> films, sputtered on adjacent Pt electrodes and covered by the polymer blend PVA·KHCO<sub>3</sub>, can be used to generate diodelike current-voltage outputs that respond to CO<sub>2</sub> gas. We have later reported similar devices that are operable in aqueous solutions. When devices based on the contact of sputtered WO<sub>3</sub> and IrO<sub>2</sub> are covered by a glucose oxidase containing polymer, they can exhibit reversible and reproducible glucose-dependent, diodelike current rectification in liquids at room temperature. We now report a new device, a Ta<sub>2</sub>O<sub>5</sub>/Al<sub>2</sub>O<sub>3</sub> surface modified 2-dimensional diode array based on the serially connected contacts of sputtered WO<sub>3</sub> and IrO<sub>2</sub>, Figs. 3, 7 and 8.

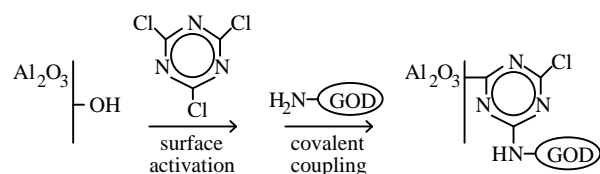
### 三、實驗方法

The Pt-pad electrodes in Fig. 3 are fabricated using similar procedures as described earlier.<sup>7)</sup> The electrodes are typically 200  $\mu\text{m}$  wide and 1,000  $\mu\text{m}$  long and are separated by a distance of 200  $\mu\text{m}$ . To avoid annealing the  $\text{IrO}_2$  due to heating by subsequent  $\text{WO}_3$  deposition, sputtering of the  $\text{WO}_3$  target (99.99%, Pure Tech) at radiofrequency is carried out first under 20%  $\text{O}_2$  in Ar at a total pressure of 90 mTorr, in the same apparatus as used before.<sup>8)</sup> A stainless-steel sheet with laser-opened holes or a Si wafer with micromachined V-grooves is used as the deposition mask. The mask and devices on the wafer are pressed onto a heated substrate platen at 676 K.<sup>4)</sup> The deposited  $\text{WO}_3$  films exhibit broad cyclic voltammograms in aqueous 1.0 M  $\text{HClO}_4$  over the potential range of 0.3 to -0.3 V vs a saturated calomel electrode, as reported previously.<sup>4)</sup> Characterization of the films on indium-tin oxide glass shows electrochromism in the visible region and a wide range of absorption change under potential cycling in aqueous 1.0 M  $\text{H}_2\text{SO}_4$ . The change is ~15-85% in transmittance at 650 nm, near the wavelength of maximum difference in the absorption band. The process for derivatizing the Pt electrodes with the amorphous  $\text{IrO}_2$  film, next to the  $\text{WO}_3$  films (Fig. 3), by the reactive sputtering method and the characterizations have been described earlier.<sup>8)</sup>

The deposition of  $\text{Ta}_2\text{O}_5$  and  $\text{Al}_2\text{O}_3$  membranes (~2-300 Å thick) is carried out by sputtering of a  $\text{Ta}_2\text{O}_5$  or  $\text{Al}_2\text{O}_3$  target (99.99%, Pure Tech) under 45%  $\text{O}_2$  in Ar at a total pressure of 100 mTorr, in the same apparatus as used before. The integrity of the sputtered  $\text{Ta}_2\text{O}_5$  or  $\text{Al}_2\text{O}_3$  membrane as a barrier to electron transport from solution redox species is tested on a flat Pt electrode. Potential cycling of the Pt/ $\text{Ta}_2\text{O}_5$  or Pt/ $\text{Al}_2\text{O}_3$  electrode in aqueous 10 mM  $\text{K}_3\text{Fe}(\text{CN})_6$  in 0.10 M KCl electrolyte has yielded no discernible cyclic voltammetric waves that are characteristic of the redox species even at the highest current sensitivity of the potentiostat (BAS CV-50W, Bioanalytical Systems). The prepared  $\text{WO}_3$ ,  $\text{IrO}_2$ ,  $\text{Ta}_2\text{O}_5$  and  $\text{Al}_2\text{O}_3$  films are robust and adhere strongly to the Pt surface. No difficulty such as peeling has been encountered throughout the course of our experiment. After deposition of the oxide films, electrical

contact of individual Pt electrodes is made using Ag epoxy, which is later encapsulated using insulating epoxy. Optical microscopy reveals that uniform bleaching and coloring can occur in each of the insertion oxide films on Pt. As shown in Fig. 3, each film has only one underlying Pt electrode. This forces the potential drop to be confined to the  $\text{WO}_3/\text{IrO}_2$  interfaces, leaving the individual films on Pt approximately at equipotential and of the same color.

In the next step, the whole device active area is covered with covalently immobilized glucose oxidase (GOD, Type VII from *Aspergillus niger*, Sigma) (Fig. 3). This enzyme layer is used for creating a glucose-modulated pH environment specifically for the diode. The procedure for the covalent immobilization of GOD is performed separately in two sequential steps:<sup>13,14)</sup>



The first step involves the activation of the exposed  $\text{Al}_2\text{O}_3$  surface (Fig. 3) by cyanuric chloride. The reason for the choice is due to the simplicity of the cyanuric chloride reaction over the other reagents. The second step involves the preparation of immobilized enzyme derivatives via covalent coupling in the presence of glucose.<sup>13,14)</sup> In order to protect the active site, it is common practice to carry out this reaction in the presence of the substrate. The reaction also needs to be performed under mild conditions. Low temperature, low ionic strength and pH in the physiological range are important factors in preventing the enzyme from denaturing. The determination of the optimal conditions for the maximum retention of enzyme activity is a trial-and-error process. Before activation, the exposed  $\text{Al}_2\text{O}_3$  surface is pretreated in aqueous 0.1 M KOH for 60 s to grow hydroxyl groups. After washing with deionized  $\text{H}_2\text{O}$  and dried, the surface is reacted with 0.05 M cyanuric chloride in benzene for 2 h at 50 °C. Before covalent coupling, GOD (1,200 units or 10 mg) is dissolved in 0.2 ml aqueous 0.1 M phosphate solution (pH 8.0) saturated with glucose. No other supporting electrolyte has been added since the enzyme layer functions only as a source or sink for  $\text{H}^+$ , and not as an

electrolyte to carry ionic current. The enzyme solution (100  $\mu$ l) is placed with a microsyringe over the exposed active area of the diode array (Fig. 3) and chilled at 4  $^{\circ}$ C for 12 h to form the non-leaching glucose oxidase enzyme layer. This covalently immobilized enzyme layer forms light-yellow films that are highly adhesive to  $\text{Al}_2\text{O}_3$ . No peeling of the films has been encountered throughout the electrical experiments. Enzyme layers immobilized with the same procedure separately on glass slides have been immersed in  $\text{H}_2\text{O}$  at 37  $^{\circ}$ C for at least 4 months without any visible sign of disintegration.

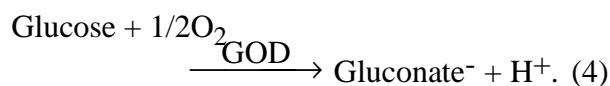
The potential of the Pt/IrO<sub>2</sub>/Ta<sub>2</sub>O<sub>5</sub> or Pt/IrO<sub>2</sub>/Al<sub>2</sub>O<sub>3</sub> electrode as a function of pH has been measured by use of a Keithley 617 electrometer. A 10 mM Britton-Robinson buffer<sup>15)</sup> solution, initially at pH  $\sim$ 0.0, is titrated with KOH in steps to generate the pH buffer solutions, reaching a final pH value of  $\sim$ 14, Fig. 1. The pH jump experiment for Ta<sub>2</sub>O<sub>5</sub> or Al<sub>2</sub>O<sub>3</sub> modified IrO<sub>2</sub> electrode in Fig. 2 is performed on a flow-injection apparatus<sup>16)</sup> that can perform fast switching between two pH buffer streams (4.0 and 7.0) of aqueous 0.1 M phosphate. The current-voltage sweeps are generated using a Keithley 236 source-measure unit (Fig. 3). The diode arrays packaged into integral flow cells are used, as earlier,<sup>16)</sup> to allow exposure to glucose solutions with different concentrations. Low concentration aqueous phosphate (10 mM, pH 7.0) buffer solution is used as the carrier for glucose to facilitate pH change in immobilized GOD. The conditions of glucose concentrations or the interfering redox species carried in the buffer solutions are generated by ratioing the flowrate of microprocessor-controlled infusion pumps (Sage 341B). Bovine meat samples are first incubated at 37  $^{\circ}$ C for 24-48 h in air to induce depletion of glucose by micro-organisms at the surface. A vertical incision is made to half the sample, which is then carefully laid onto the microsensor with the incised surface pressed against the array, Fig. 8.

#### 四、結果與討論

Experiments show that neither the surface modification by Ta<sub>2</sub>O<sub>5</sub> or Al<sub>2</sub>O<sub>3</sub> nor redox interference has affected the electrochemistry of IrO<sub>2</sub>, Fig. 1. A burst of O<sub>2</sub> gas is purged through the solution every other 3 min as a source of redox interference.

The potential developed on Ta<sub>2</sub>O<sub>5</sub> or Al<sub>2</sub>O<sub>3</sub> modified IrO<sub>2</sub> electrodes toward H<sup>+</sup> still exhibit Nernstian behavior as before ( $E^{\circ}$  is  $\sim$ -0.73 V vs Ag/AgCl, and  $\Delta E^{\circ}$  is -59 mV per  $\Delta$ pH in either case). This shows that Ta<sub>2</sub>O<sub>5</sub> or Al<sub>2</sub>O<sub>3</sub> can block electron transfer from solution redox species in (1) as expected. Moreover, the valid dynamic range for Al<sub>2</sub>O<sub>3</sub> is found to be within pH 0-14, which is larger than the pH 2-12 for Ta<sub>2</sub>O<sub>5</sub>, Fig. 1. When pH-jump experiment for Ta<sub>2</sub>O<sub>5</sub> or Al<sub>2</sub>O<sub>3</sub> modified IrO<sub>2</sub> electrode is performed, Fig. 2, the Al<sub>2</sub>O<sub>3</sub> under test shows a faster response toward pH change than Ta<sub>2</sub>O<sub>5</sub> (both 200  $\text{\AA}$  thick) by a factor of  $\sim$ 5.

The glucose-dependent current-voltage characteristics of a single Ta<sub>2</sub>O<sub>5</sub>/Al<sub>2</sub>O<sub>3</sub> modified diode on the 5-diode array based on WO<sub>3</sub> and IrO<sub>2</sub> are shown in Fig. 4. The glucose creates a pH-regulated environment for the diodes (Fig. 3), through its pH-lowering effect, as previously reported.<sup>17)</sup> Glucose equilibration catalyzed by the immobilized glucose oxidase proceeds according to the reaction



As results of the glucose-dependent experiment in Fig. 4 show, diodes based on WO<sub>3</sub> and IrO<sub>2</sub> undergo a current decrease in the forward direction when the glucose concentration is increased within the range of 0.2-10 mM in phosphate buffer solutions. This result is consistent with the WO<sub>3</sub> and IrO<sub>2</sub> redox processes (reactions (2) and (3)). The electrochemical potentials in both reactions become more positive in more acidic environments. This shift can be considered to result from the pH-dependent changes in the potential drop across the Helmholtz layer at the surface of both oxides, as stated earlier.<sup>7,8)</sup> On the potential scale, the shifting of redox potentials towards the positive region renders reductions more favorable than oxidations under fixed driving force. When the bias voltage is unchanged, the current passing through a less fully oxidized IrO<sub>2</sub> in series with a more fully reduced H<sub>x</sub>WO<sub>3</sub> in the forward direction still shows a loss due to the current-limiting effect exerted by the higher resistance (Fig. 4). The fact that the experimentally determined pH sensitivity for our IrO<sub>2</sub> ( $\sim$ 58 mV/ $\Delta$ pH) in aqueous solutions,<sup>8)</sup> is higher than that for our WO<sub>3</sub> ( $\sim$ 52 to 54 mV/ $\Delta$ pH), is relevant

and should be noted. This means that up to ~5 mV/ $\Delta$ pH positive displacement of IrO<sub>2</sub> potential in excess of that of WO<sub>3</sub> can be expected in the more acidic diode environments created by glucose. That should further contribute to the current loss in the forward direction. The current loss in Fig. 4 in the forward direction is also confirmed by the observed progressive coloration in H<sub>x</sub>WO<sub>3</sub> and discoloration in IrO<sub>2</sub> as the pH is lowered in the immobilized GOD layer by glucose solution under a fixed positive bias.

The new Ta<sub>2</sub>O<sub>5</sub>/Al<sub>2</sub>O<sub>3</sub> modified diodes are markedly durable and reproducible. Repeated voltage sweeps under each glucose concentration in Fig. 4 give almost identical current-voltage signals. Neither the rectification behavior nor the current amplitudes show signs of degradation. Under a fixed 1.6 V bias, switching the solution between 0.2 to 10 mM glucose in phosphate buffer turns the new diodes to the "on" and "off" states (Fig. 5). They exhibit ~-(5 to 20)  $\mu$ A and 0  $\mu$ A current change in the forward direction, respectively (Fig. 6). The current switchings are free of interference from injected O<sub>2</sub> solutions, reversible and reproducible and can be carried out for all diodes on the array without significant deterioration for >36 h.

The sensitivity or dynamic range of the Ta<sub>2</sub>O<sub>5</sub>/Al<sub>2</sub>O<sub>3</sub> modified diodes on the array for glucose concentration is found to be dependent on the pH value of the carrier buffer solution used. Glucose is capable of inducing a larger pH drop in immobilized GOD layer when the buffer solution is more basic. As shown in Fig. 6, the Ta<sub>2</sub>O<sub>5</sub>/Al<sub>2</sub>O<sub>3</sub> modified diodes have a valid range for glucose concentrations between ~0.2-10 mM. Separate experiments show that the diodes can actually respond to glucose from 60 to 0.01 mM with acceptable signal-to-noise ratio. It has also been determined that the glucose-induced current change in the forward direction is proportional to the logarithm of the glucose concentration to which immobilized GOD is exposed, as shown in the inset in Fig. 6.

Next, experiments are performed on the newly constructed Ta<sub>2</sub>O<sub>5</sub>/Al<sub>2</sub>O<sub>3</sub> modified 4 x 5 diode array. Figure 7 shows the layout and numbering scheme of the new array. The experiments demonstrate that the new 4 x 5 diode array is capable of resolving the 2-dimensional spatial distribution of glucose concentration in food material in uncontrolled air atmosphere with changing oxygen content.

A bovine tissue incubated for bacterial growth at the surface (controlled at 37 °C in air for 24 h) is placed over the array, Fig. 8. The diodes on the array, each biased individually, show spatially resolved rectifying I-V characteristics, Figs. 9-10. The detected forward currents at 1.6 V bias in Fig. 9 produce a 2-dimensional 4 x 5 image of the blood glucose distribution that has been generated by the surface-to-bulk bacterial consumption near the tissue surface. Since glucose is progressively depleted from the surface as a function of time, this result can be used to build a quantitative database on the sensing of freshness<sup>18)</sup> in food materials. In particular, the new 4 x 5 diode array has a potential for practical use as a microsensor for acquiring the "freshness images" of foods in the air.

This work reveals that oxide-based microsensors are durable and that, in principle, many oxides with widely varying properties can be used to fabricate sensing devices with special electrical characteristics. In addition, functions can be readily built-in to suppress interference and enhance reliability. Work is already under way, in this laboratory, to incorporate this diode in other microsensors. Other details of the device can be found in Ref. 19.<sup>19)</sup>

## 五、計畫成果自評

本研究內容與原計畫相符程度約95%。達成預期目標，包括創新元件之發現、其理論之推導和模式建立、所用實驗原型和系統之建立、以及人才培育等。本研究結果具有學術、應用價值，可發表於國外期刊和申請專利。本研究主要發現，包括以獨具的整流機制，建構感測用二極體元件，並以表面修飾，阻擋干擾源、賦予元件關鍵的抗干擾特質、耐久性和可靠性。以這種元件為基礎，可以發展出其他二極體的陣列微感測器，能用於各種生物液體中，獲得生物分子的空間分佈資訊，並向感測資訊影像化邁進。這是應用傳統二極體建立微感測器無法做到的。

## 六、參考文獻

- 1) T. A. Fjeldly and K. Nagy: J. Electrochem. Soc., **127** (1980) 1299.
- 2) M. O. Schloh, N. Leventis and M. S. Wrighton: J. Appl. Phys. **66** (1989) 965.
- 3) B. Scrosati: *Applications of Electroactive Polymers*, ed. B. Scrosati (Chapman & Hall, London, 1993) p. 256.
- 4) M. J. Natan, T. E. Mallouk and M. S.

- Wrighton: *J. Phys. Chem.* **91** (1987) 648.
- 5) K. Paztor, A. Sekiguchi, N. Shimo, N. Kitamura and H. Masuhara: *Sens. & Actuat. B* **12** (1993) 231.
  - 6) M. J. Natan and M. S. Wrighton: *Prog. Inorg. Chem.* **37** (1989) 391.
  - 7) S. Chao: *Jpn. J. Appl. Phys.* **32** (1993) L1346.
  - 8) J. C. Lue and S. Chao: *Jpn. J. Appl. Phys.* **36** (1997) 2292.
  - 9) J. W. Gardner: *Microsensors, Principles and Applications* (John Wiley, Chichester, 1994) p. 235.
  - 10) R. D. Rauh and S. F. Cogan: *J. Electrochem. Soc.* **140** (1993) 378.
  - 11) N. Leventis, M. O. Schloh, M. J. Natan, J. J. Hickman and M. S. Wrighton: *Chem. Mater.* **2** (1990) 568.
  - 12) S. Chao: *Jpn. J. Appl. Phys., Part 2*, **37** (1998) 245.
  - 13) P. W. Carr and L. D. Bowers: *Immobilized Enzymes in Analytical and Clinical Chemistry* (J. Wiley & Sons, New York, 1980).
  - 14) B. Eggins: *Biosensors* (Wiley Teubner, Chichester, 1996) p. 37.
  - 15) J. A. Dean: *Lange's Handbook of Chemistry* (McGraw-Hill, New York, 1992) p. 109.
  - 16) S. Chao: *Meas. Sci. Technol.* **7** (1996) 737.
  - 17) Y. Hanazato, M. Nakako and S. Shiono: *IEEE Trans. Electron Devices* **33** (1986) 47.
  - 18) *Sensor Review*, **9** (1989) 15.
  - 19) C. C. Hsu and C. C. Lin: M. S. Thesis, Dept. Electrophys., NCTU, 1999.
  - 20) D. Sawyer, A. Sobkowiak and J. L. Roberts: *Electrochemistry for Chemists* (Wiley, New York, 1995) p. 199.

## 七、圖表

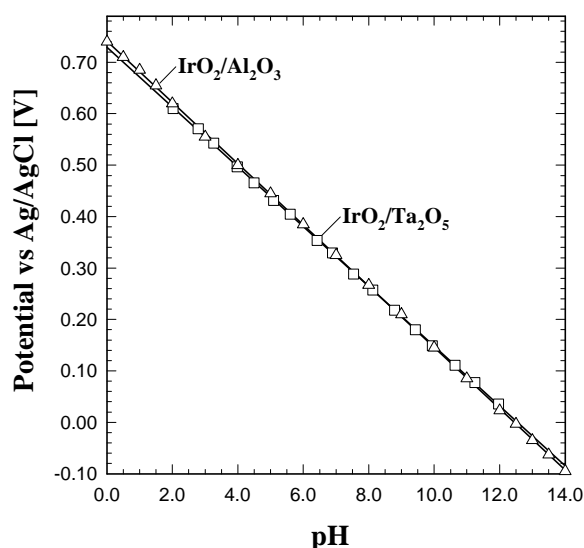


Fig. 1. Nernstian potential developed on  $\text{Ta}_2\text{O}_5$  or  $\text{Al}_2\text{O}_3$  modified  $\text{IrO}_2$  electrode toward  $\text{H}^+$  ( $E^0$  is  $\sim 0.73$  V vs Ag/AgCl,  $\Delta E^0$  is  $-59$  mV per  $\Delta\text{pH}$  in either case). A burst of  $\text{O}_2$  is purged through the solution every other 3 min as a source of redox interference. Neither the modification nor the interference has affected the electrochemistry of  $\text{IrO}_2$ . The dynamic range for  $\text{Al}_2\text{O}_3$  is pH 0-14, which is larger than pH 2-12 for  $\text{Ta}_2\text{O}_5$ .

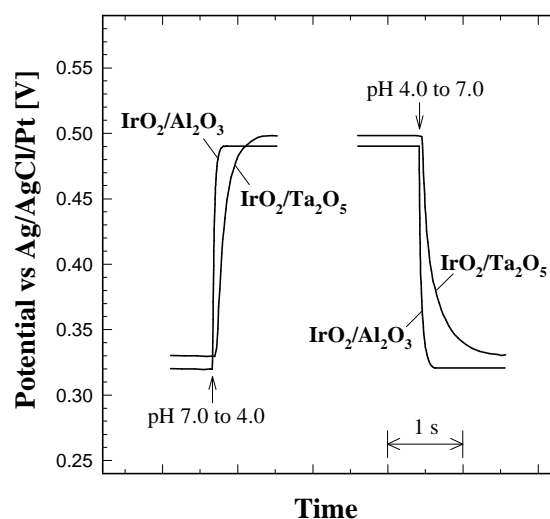


Fig. 2. A pH-jump experiment for  $\text{Ta}_2\text{O}_5$  or  $\text{Al}_2\text{O}_3$  modified  $\text{IrO}_2$  electrode, showing that  $\text{Al}_2\text{O}_3$  is faster responsive than  $\text{Ta}_2\text{O}_5$  (both 200 Å thick) by a factor of  $\sim 5$ . The Ag/AgCl/Pt used is a reference electrode for fast electrochemistry.<sup>20)</sup>

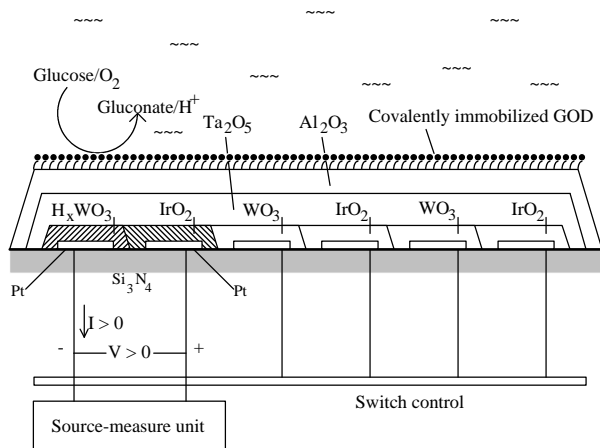


Fig. 3. Scheme showing the  $\text{Ta}_2\text{O}_5/\text{Al}_2\text{O}_3$  surface modified diode array and one forward-biased diode based on the contact of  $\text{WO}_3$  and  $\text{IrO}_2$  on Si under glucose modulation in  $\text{H}_2\text{O}$ .

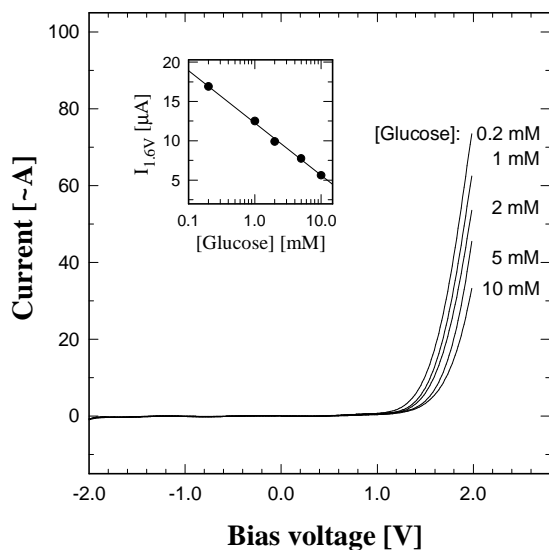


Fig. 4. Typical single diode current-voltage characteristics on a  $\text{Ta}_2\text{O}_5/\text{Al}_2\text{O}_3$  modified, 5-diode array (Fig. 3) under the modulation of glucose concentrations in phosphate buffer at 298 K.

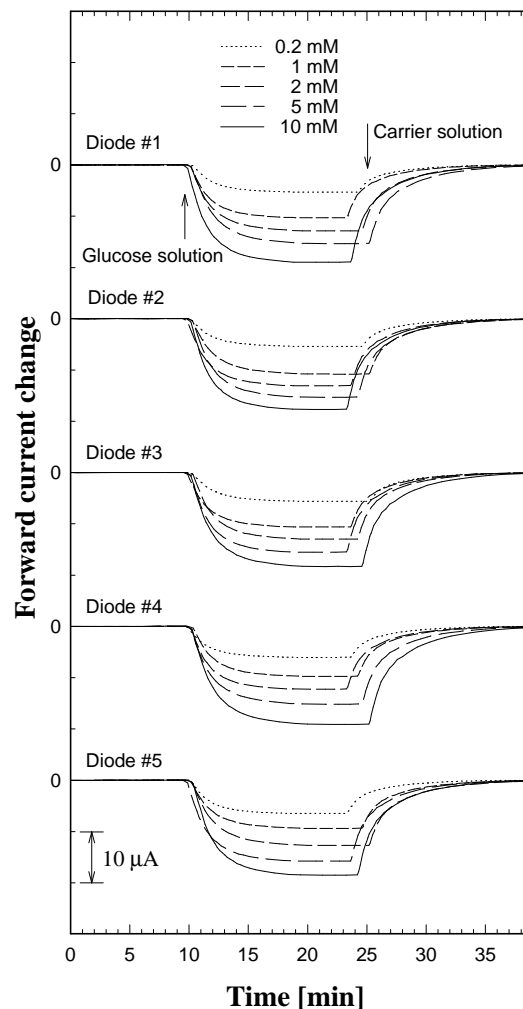


Fig. 5. Typical interference-free electrical response of a  $\text{Ta}_2\text{O}_5/\text{Al}_2\text{O}_3$  modified, 5-diode array. The glucose concentration-induced switching behaviors of each diode are produced under a forward bias of 1.6 V at 298 K. The carrier flows are 10 mM aqueous phosphate buffer solution adjusted to pH 7.0. The source of redox interference is a burst of 0.2 ml  $\text{O}_2$ -saturated  $\text{H}_2\text{O}$ , injected every 2 min into the carrier flow.



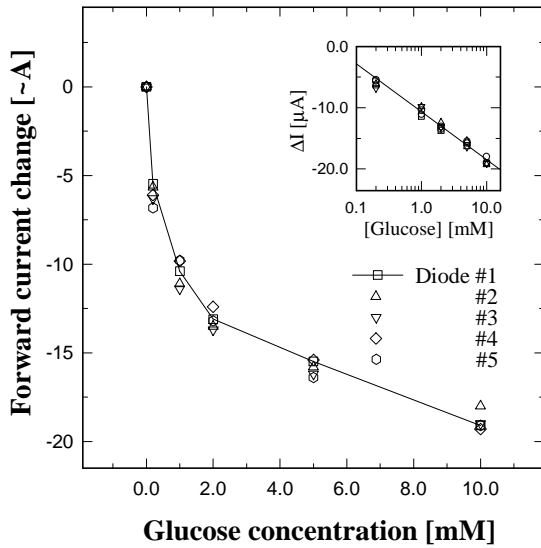


Fig. 6. Typical current changes in the forward direction (1.6 V bias) of a Ta<sub>2</sub>O<sub>5</sub>/Al<sub>2</sub>O<sub>3</sub> modified, 5-diode array induced by glucose concentrations in phosphate buffer at pH 7.0 and 298 K.

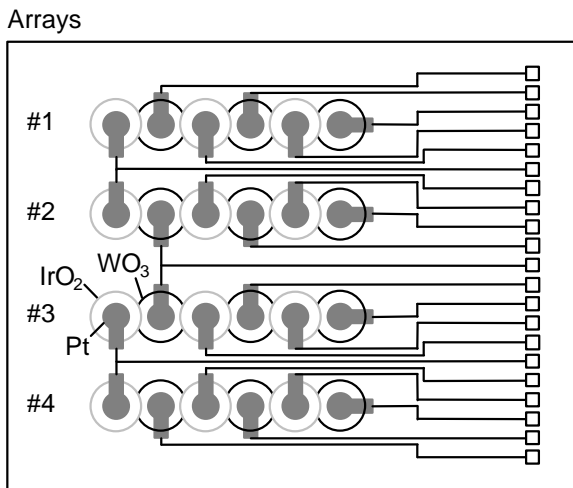


Fig. 7. Typical layout and numbering scheme of the 4 x 5 diode array based on the contact of WO<sub>3</sub> and IrO<sub>2</sub> on Si.

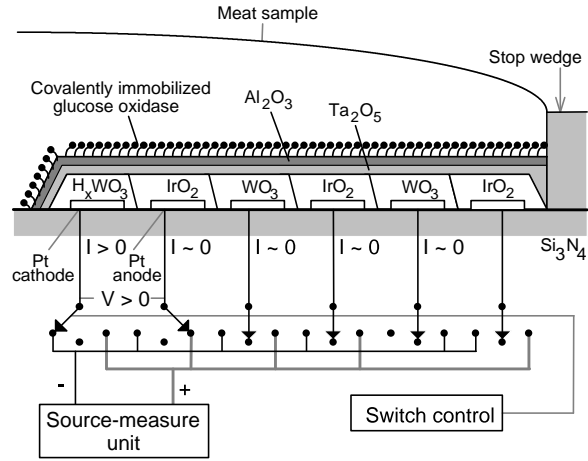


Fig. 8. Side-view of the Ta<sub>2</sub>O<sub>5</sub>/Al<sub>2</sub>O<sub>3</sub> surface modified 4 x 5 diode array, one forward-biased diode based on the contact of WO<sub>3</sub> and IrO<sub>2</sub> on Si, and the incubated meat sample measurement scheme.

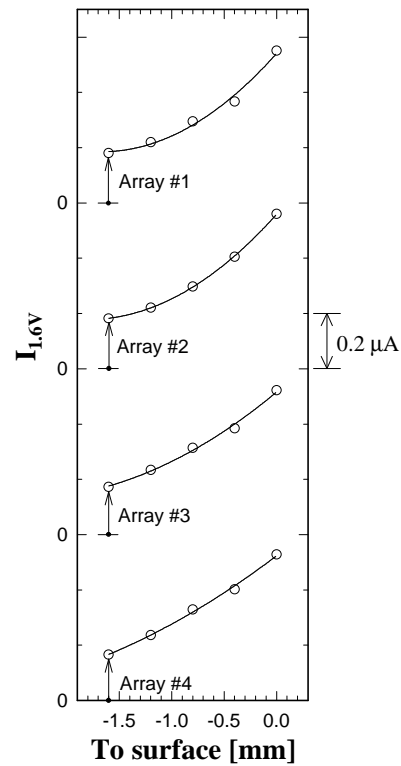


Fig. 9. Typical spatially resolved current in the forward direction (1.6 V bias) of a Ta<sub>2</sub>O<sub>5</sub>/Al<sub>2</sub>O<sub>3</sub> modified, 4 x 5 diode array induced by the glucose concentration gradient in an incubated meat sample at 298 K in uncontrolled air atmosphere. (Diodes are labeled by their distance to the incubation surface, Fig. 7).

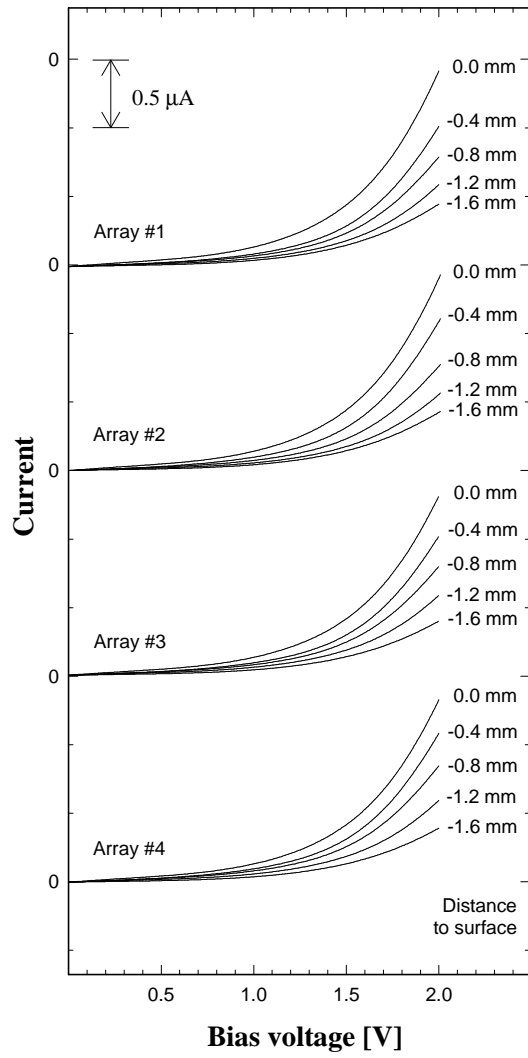


Fig. 10. Forward current-voltage data of the 4 x 5 diode array in Fig. 9.